CHEMPHYSCHEM

Supporting Information

Regional Susceptibility in VCD Spectra to Dynamic Molecular Motions: The Case of a Benzyl α-Hydroxysilane**

Yiyin Xia[+],[a] Mark A. J. Koenis[+],[a] Juan F. Collados,[b] Pablo Ortiz,[b] Syuzanna R. Harutyunyan,[b] Lucas Visscher,[c] Wybren J. Buma,[a] and Valentin P. Nicu*[a, d]

cphc_201701335_sm_miscellaneous_information.pdf

1 Experimental and Computational details

1.1 Experimental details

Both enantiomers of 3-methyl-1-(methyldiphenylsilyl)-1-phenylbutan-1-ol (silyl alcohol) were synthesized with an enantiomeric excess of over 90% as discribed in reference [1]. Fourier-Transform InfraRed (FTIR) absorption and VCD spectra were obtained by using a Bruker Vertex 70 spectrometer in combination with a PMA 50 module for polarization modulation measurements. The PEM center frequency PEM was set to 1400 cm^{-1}. A CaF transmission cell with a path length of 50 μm was used. To account for the differences in extinction coefficients a 1.0 M sample was used for recording the 950 cm^{-1} to 1140 cm^{-1} region, while a 1.9 M sample was employed for the 1140 cm^{-1} to 1650 cm^{-1} region. The baseline correction for both IR and VCD spectra was performed using the spectra of deuterated chloroform.

1.2 Computational details

Geometry optimisations, IR absorption and VCD calculations have been performed using the ADF program [2–4]. To assess the influence of the choice of computational parameters several additional calculations have been performed. For the 23 low-energy conformers geometry optimization and VCD calculations have been performed at the OLYP/TZP and PBE/TZP level of theory[5–7]. Additionally, solvent effects have been studied using the COSMO solvation model of chloroform at a BP86/TZP level of theory [8, 9]. Calculations have also been performed at the BP86/TZP level of theory including the D3-BJ dispersion correction [10]. Since the relative energies of the conformers computed with the dispersion term were found to be significantly different from the standard calculations, all other generated conformers originally found to be within 10 kcal/mol have been optimized with these parameters as well. This resulted in 30 conformations within 2 kcal·mol^{-1} for which the VCD spectra have been computed.

The computed frequencies have been uniformly scaled with factor 1.009. The IR and VCD spectra were generated by convolving the line spectrum with a Lorentzian function with a half width of 8 cm^{-1}. The spectra from the individual conformers and from the different LT steps have been combined using Boltzmann weights based on the computed relative energies and a temperature of 293 K. The computed VCD spectra have been analyzed with the General Coupled Oscilator (GCO) analysis method [11]. For the rotational strength decomposition the molecule was split into a fragment containing the OH group and a fragment containing the rest of the molecule. During the linear transit calculations some important normal modes were tracked from structure to structure by calculating overlaps between the normal modes using the same methodology as described in reference [12].

1.2.1 Conformational search

First, a molecular mechanics (MM) conformational search was performed with the MacroModel module from the Schrödinger software package using the Merck Molecular Force Field (MMFF) [13–15]. 10000 conformers were generated using the mixed torsional and low-mode sampling. The energy cutoff was set to 10 kcal/mol and optimized conformers were filtered using a maximum atom deviation cutoff of 0.5 Å, leading to 107 conformers. To ensure that no conformers had been overlooked a second conformational search was performed with the RDKit software available in the Amsterdam Density Functional (ADF) software suite [16, 17]. Also in RDKit 10000 conformers were generated using a filter of 0.2 RMS. The generated conformers were optimized with MM using the UFF force field and subsequently filtered employing an RMS filter of 0.1 [18]. This resulted in another 256 conformers with energies within 10 kcal/mol.

The generated conformers from Macromodel and RDKit were optimized with DFT using the QUILD optimization routines in the ADF software suite using the BP86 functional and and TZP basis set [2, 3, 19–22]. The resulting conformers were checked for duplicates with an in-house code that used a maximum atom-to-atom distance deviation of 0.5 Å. This resulted in 20 and 23 conformers within 2.00 kcal·mol^{-1} for the starting conformers from Macromodel and RDKit, respectively. The three additional conformers found with RDKit have a relatively high energy (1.76, 1.85 and 1.96 kcal·mol^{-1}). The fact the MacroModel and RDKit have made similar predictions assures us that we have considered the most relevant low-energy conformations.

1.2.2 Linear transit calculation

Linear transit (LT) calculations have been performed with ADF changing either an angle or a dihedral angle from the equilibrium geometry of the conformer of interest. In Fig. S4 an overview is shown of all the different LT calculations. These LT calculations have only been done for the two lowest-energy conformers (8 and 10). For the LT calculation scanning the C-O-H angle all conformers have been considered as this angle was found to have the largest effects on the VCD spectra. In the LT calculations angles have been changed in both directions in 15 steps of 1° and dihedral angles in 18 steps of 5°. At each LT step the other structural parameters were reoptimized using the standard ADF optimization routines. For LT structures within 1 kcal·mol^{-1} IR and VCD spectra have been calculated with ADF.

2 General coupled oscillator analysis

According to the General Coupled Oscillator (GCO) analysis [11], by dividing a molecule into two fragments **A** and **B**, the rotational strength (R_{01}) of a given mode can be split in a contribution from the two individual fragments ($R_{01}^{\mathbf{IF}}$) and a GCO contribution ($R_{01}^{\mathbf{GCO}}$) representing the interaction between the two fragments:

$$R_{01}(j) = R_{01}^{\mathbf{IF}}(j) + R_{01}^{\mathbf{GCO}}(j) \tag{1}$$

with

$$R_{01}^{\mathbf{IF}}(j) = -i \cdot \left[\vec{E}_{01}^{\mathbf{A}}(j) \cdot \vec{M}_{10}^{\mathbf{A}}(j) + \vec{E}_{01}^{\mathbf{B}}(j) \cdot \vec{M}_{10}^{\mathbf{B}}(j) \right], \tag{2}$$

$$R_{01}^{\mathbf{GCO}}(j) = -i \cdot \left[\vec{E}_{01}^{\mathbf{A}}(j) \cdot \vec{M}_{10}^{\mathbf{B}}(j) + \vec{E}_{01}^{\mathbf{B}}(j) \cdot \vec{M}_{10}^{\mathbf{A}}(j) \right] \tag{3}$$

Here $\vec{E}_{01}^{\mathbf{X}}(j)$ and $\vec{M}_{01}^{\mathbf{X}}(j)$ with $\mathbf{X} = (\mathbf{A}, \mathbf{B})$ are the electric and magnetic dipole transition moments associated with the molecular fragments.

Such a decomposition provides insight into the magnitude and stability of the computed VCD intensities [23]. Table S1 lists the results of the GCO analysis performed for the intense VCD bands observed in the frequency interval between 1150 and 1360 cm^{-1} in the VCD spectra computed for conformers 8 and 10. This demonstrates that the rotational strengths of these bands are essentially determined by the orientation and magnitude of the electric dipole transition moment of the hydroxyl group. The GCO decomposition was performed using the hydroxyl group as fragment **A**, and the rest of the atoms in the molecule as fragment **B**.

Conformer	Mode	Frequency	R_{01}	$R_{01}^{\mathbf{GCO}}$	$R_{01}^{\mathbf{IF}}$
8	92	1155.6	−20.22	−27.17	+6.95
8	107	1340.4	+54.79	+66.37	−11.58
10	101	1294.6	−30.33	−28.84	−1.49
10	102	1306.0	−48.72	−52.80	−4.08
10	107	1336.3	+20.95	+45.27	−24.32

Table S1: GCO analysis of the intense bands observed in the OH-bending region of the VCD spectra computed for conformers 8 and 10. The frequency is given in cm^{-1} and the rotational strength (R_{01}) and its components in $10^{-44} esu^2 \cdot cm^2$.

3 Figures

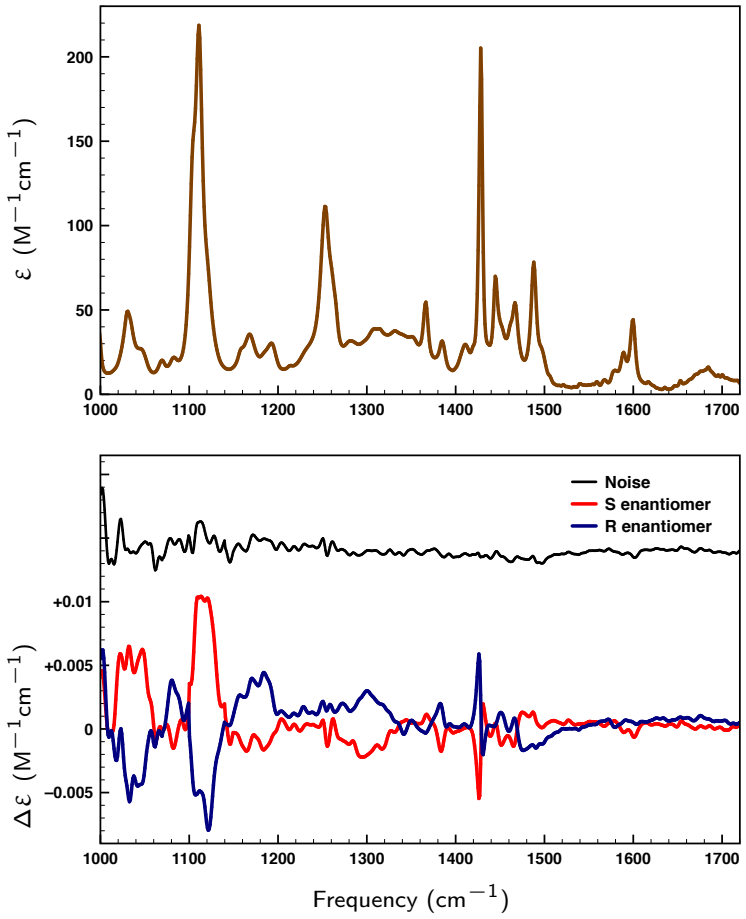

Figure S1: Experimental IR absorption and VCD spectra of 3-methyl-1-(methyldiphenylsilyl)-1-phenylbutan-1-ol (silyl-alcohol). The noise of the VCD spectrum has been calculated as half of the sum of the VCD spectra of the two enantiomers.

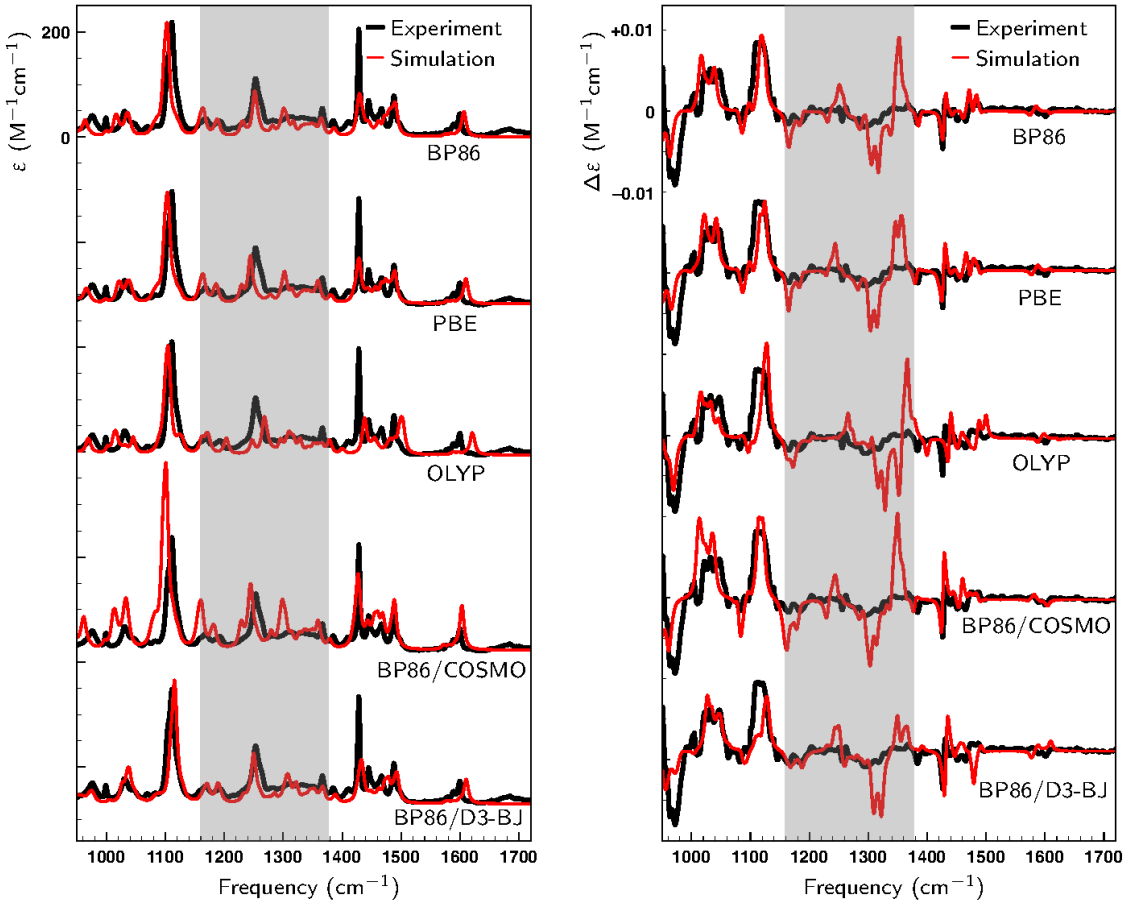

Figure S2: Comparison between simulated and experimental IR absorption (left) and VCD (right) spectra using different computational parameters: BP86/TZP, PBE/TZP, OLYP/TZP, COSMO solvation model for chloroform with BP86/TZP, and BP86/TZP with the DTF-D3-BJ dispersion correction term.

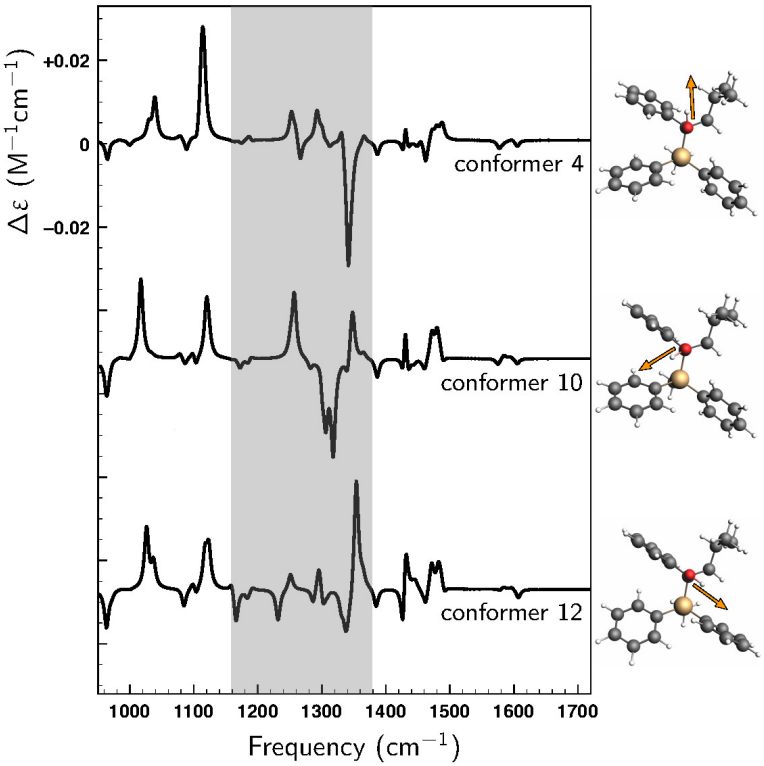

Figure S3: Comparison between predicted VCD spectra of conformers 4, 10 and 12 which differ primarily in the orientation of the OH-bond.

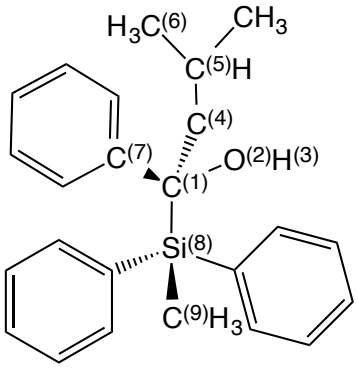

Linear Transit Parameters

LT1: $\angle\, C^{(1)}O^{(2)}H^{(3)}$
LT2: $\angle\, C^{(1)}Si^{(8)}C^{(9)}$
LT3: $\angle\, C^{(4)}C^{(1)}Si^{(8)}$
LT4: $\angle\, C^{(6)}C^{(1)}C^{(9)}$
LT5: $\angle\, C^{(7)}C^{(1)}O^{(2)}$
LT6: $\angle\, C^{(7)}C^{(1)}C^{(4)}$
LT7: $\angle\, C^{(7)}C^{(1)}C^{(5)}$
LT8: $\angle\, Si^{(8)}C^{(1)}O^{(2)}$
LT9: $\angle\, C^{(1)}C^{(4)}C^{(5)}C^{(6)}$
LT10: $\angle\, O^{(2)}C^{(1)}Si^{(8)}C^{(9)}$
LT11: $\angle\, C^{(4)}C^{(1)}O^{(2)}H^{(3)}$
LT12: $\angle\, Si^{(8)}C^{(1)}C^{(4)}C^{(5)}$

Figure S4: Scheme of S-3-methyl-1-(methyldiphenylsilyl)-1-phenylbutan-1-ol with a list of explored linear transit parameters.

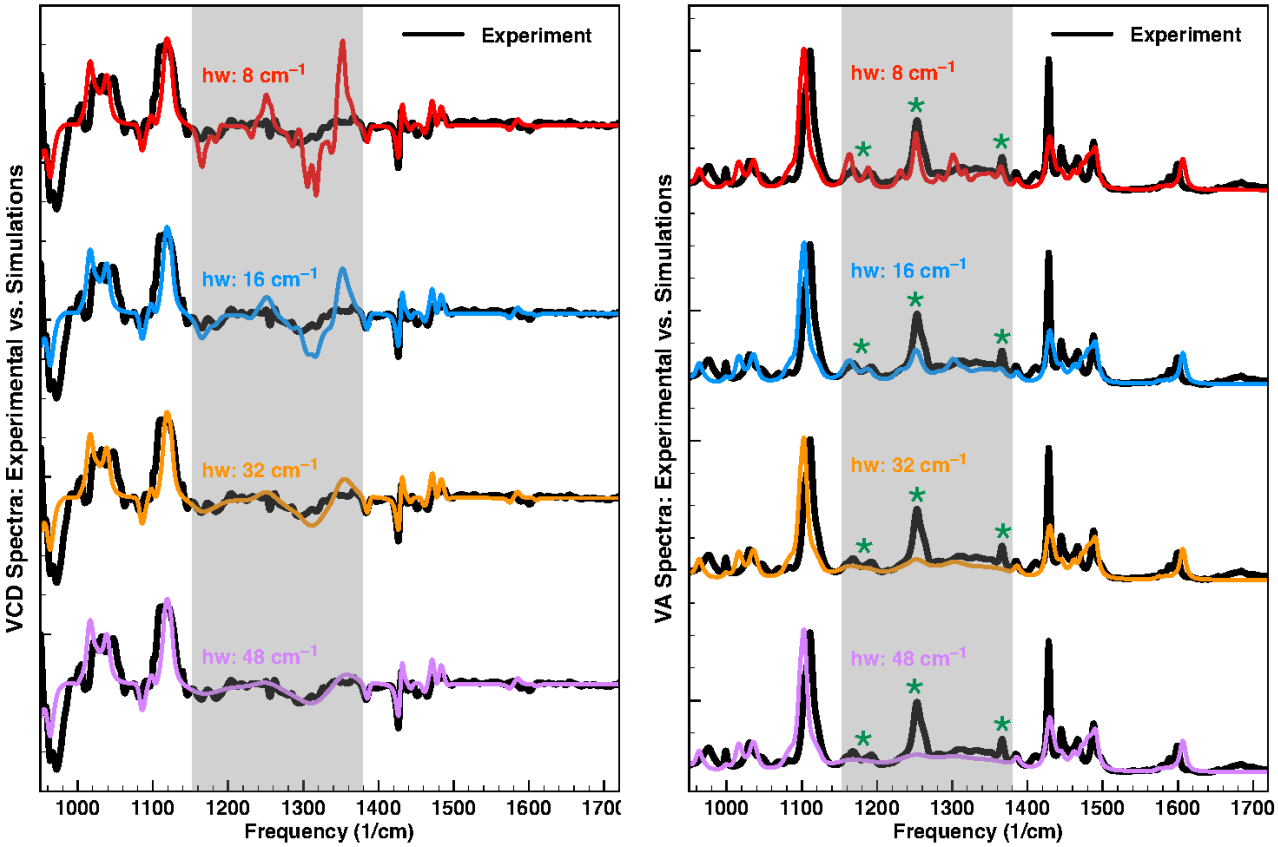

Figure S5: Comparison of experimental (black) and simulated (coloured) VCD and VA spectra. The various simulated spectra have been obtained by broadening the bands in the problematic spectral region (1160 – 1380 cm^{-1}) with Lorentzian band shapes of different half-widths, i.e., 8 cm^{-1} (red), 16 cm^{-1} (light blue), 32 cm^{-1} (orange), and 48 cm^{-1} (purple). The bands outside the 1160 – 1380 cm^{-1} spectra region have been broadened using Lorentzian band shapes with a half-width of 8 cm^{-1}. As can be seen, by increasing the half-width value the agreement between experimental and simulated spectra is improved in the case of VCD, while in the case of VA it is deteriorated (see the bands highlighted by the green stars).

References

[1] J. F. Collados, P. Ortiz, Y. Xia, M. A. J. Koenis, V. P. Nicu, W. J. Buma and S. R. Harutyunyan, *Eur. J. Org. Chem.*, in press (2017).

[2] G. T. Velde, F. M. Bickelhaupt, E. J. Baerends, C. F. Guerra, S. J. A. V. Gisbergen, J. G. Snijders and T. Ziegler, *J. Comput. Chem.*, 2001, **22**, 931–967.

[3] C. F. Guerra, J. Snijders, G. te Velde and E. Baerends, *Theor. Chem. Acc.*, 1998, **99**, 391–403.

[4] V. P. Nicu, J. Neugebauer, S. K. Wolff and E. J. Baerends, *Theor. Chem. Acc.*, 2008, **119 (1-3)**, 245–263.

[5] N. C. Handy and A. J. Cohen, *Mol. Phys.*, 2001, **99**, 403–412.

[6] F. A. Hamprecht, A. J. Cohen and N. C. Handy, *J. Chem. Phys.*, 1988, **109**, 6264–6271.

[7] J. P. Perdew, K. Burke and M. Ernzerhof, *Phys. Rev. Lett.*, 1996, **77**, 3865–3868.

[8] C. C. Pye and T. Ziegler, *Theor. Chem. Acc.*, 1999, **101**, 396–408.

[9] A. Klamt and G. Schüürmann, *J. Chem. Soc., Perkin Trans. 2*, 1993, 799–805.

[10] S. Grimme, S. Ehrlich and L. Goerigk, *J. Comput. Chem.*, 2011, **32**, 1456–1465.

[11] V. P. Nicu, *Phys. Chem. Chem. Phys.*, 2016, **18**, 21202–21212.

[12] V. P. Nicu, E. Debie, W. Herrebout, B. V. D. Veken, P. Bultinck and E. J. Baerends, *Chirality*, 2010, **21**, E287–E297.

[13] *Schrödinger LLC, 2009*, http://www.schrodinger.com.

[14] F. Mohamadi, N. G. J. Richards, W. C. Guida, R. Liskamp, M. Lipton, C. Caufield, G. Chang, T. Hendrickson and W. C. Still, *J. Comput. Chem*, 1990, **11**, 440–467.

[15] T. A. Halgren, *J. Comput. Chem*, 1996, **17**, 490–519.

[16] *RDKIT: Open-source cheminformatics*, http://www.rdkit.org (accessed March 6, 2017).

[17] *Amsterdam Density Functional program*, http://www.scm.com.

[18] A. K. Rappé, C. J. Casewit, K. S. Colwell, W. Goddard III and W. M. Skiff, *J. Am. Chem. Soc.*, 1992, **114**, 10024–10035.

[19] M. Swart and F. M. Bickelhaupt, *J. Comput. Chem*, 2007, **29**, 724–734.

[20] A. D. Becke, *Phys. Rev. A*, 1988, **38**, 3098–3100.

[21] J. P. Perdew, *Phys. Rev. B*, 1986, **33**, 8822–8824.

[22] E. Van Lenthe and E. J. Baerends, *J. Comput. Chem.*, 2003, **24**, 1142–1156.

[23] V. P. Nicu, *Phys. Chem. Chem. Phys.*, 2016, **18**, 21213–21225.